Solvothermal synthesis of new metal organic framework structures in the zinc–terephthalic acid–dimethyl formamide system

ARTICLE *in* JOURNAL OF SOLID STATE CHEMISTRY · NOVEMBER 2005

Impact Factor: 2.13 · DOI: 10.1016/j.jssc.2005.08.013

Available online at www.sciencedirect.com
SCIENCE DIRECT®
Journal of Solid State Chemistry 178 (2005) 3342–3351
JOURNAL OF SOLID STATE CHEMISTRY
www.elsevier.com/locate/jssc

Solvothermal synthesis of new metal organic framework structures in the zinc–terephthalic acid–dimethyl formamide system

Henrik Fanø Clausen[a], Rasmus Damgaard Poulsen[a], Andrew D. Bond[b], Marie-Agnes S. Chevallier[a], Bo Brummerstedt Iversen[a,*]

[a]Department of Chemistry, University of Aarhus, Langelandsgade 140, 8000 Aarhus C, Denmark
[b]Department of Chemistry, University of Southern Denmark, Campusvej 55, 5230 Odense M, Denmark

Received 23 June 2005; received in revised form 17 August 2005; accepted 18 August 2005
Available online 27 September 2005

Abstract

Two new metal organic framework (MOF) structures have been obtained from the Zn–terephthalic acid (H_2BDC)–dimethyl formamide (DMF) system and examined by single-crystal X-ray diffraction: $Zn(C_8H_4O_4)(C_3H_7NO)$, **1**, monoclinic $C2/m$, $a = 11.1369(5)$, $b = 14.0217(7)$, $c = 7.9890(4)$ Å, $\beta = 106.316(1)^\circ$, $V = 1197.3(1)$ Å^3, $T = 180(2)$ K, $Z = 4$, $R_1 = 0.060$, w$R_2 = 0.169$, $S = 1.27$; $Zn(HCO_2)_3(C_2H_8N)$, **2**, trigonal $R\bar{3}c$, $a = 8.1818(1)$, $c = 22.1235(7)$ Å, $V = 1282.57(5)$ Å^3, $T = 180(2)$ K, $Z = 6$, $R_1 = 0.014$, w$R_2 = 0.039$, $S = 1.11$. Contrary to previously published structures in the same system, the crystals were obtained by solvothermal synthesis at 381 K. Structure **1** consists of 2-D layers stacked in an offset manner to accommodate DMF moieties coordinated to Zn^{2+} within voids in adjacent layers. Structure **2** consists of a 3-D network constructed from Zn^{2+} ions bridged by deprotonated formic acid moieties. Over time, the structure of **1** rearranges to $Zn(C_8H_4O_4)(C_3H_7NO)(H_2O)$ [monoclinic $P2_1/n$, $a = 6.6456(2)$, $b = 15.2232(5)$, $c = 12.6148(4)$ Å, $\beta = 104.110(2)^\circ$, $V = 1237.70(7)$ Å^3, $T = 100(2)$ K, $Z = 4$, $R_1 = 0.048$, w$R_2 = 0.100$, $S = 1.07$], which is identical to the known MOF-2 structure, obtained by crystallization at ambient conditions. The three structures were determined from crystals with similar crystal habits picked from a single solvothermal synthesis batch. The study demonstrates that MOF syntheses can give not only multiple crystal structures under different conditions, but also that numerous different structures, including some that are metastable, can be formed under identical conditions.

Keywords: Nanoporous structures; Metal organic frameworks; Solvothermal synthesis; X-ray diffraction

1. Introduction

Synthesis and characterization of nanoporous metal organic frameworks (MOFs) has spurred considerable interest [1–6]. The very attractive feature of MOFs compared to zeolites, e.g., is that the basic molecular building blocks (reactants) are preserved in the final assembled network. This offers the possibility for designing networks, where both pore size and physical/chemical properties can be manipulated by suitable selection of the basic components. Numerous MOF materials have been synthesized and characterized with an amazing variety of 1-D, 2-D and 3-D structural characteristics [1–6]. One major focus of the MOF activities has been the possibility for using the huge open volume in the nanoporous voids for gas storage. As an example, Yaghi and co-workers [7–9] have reported a series of zinc-based 3-D cubic MOFs with pore volumes exceeding those of zeolites and promising gas-storage capabilities.

In our group, focus has been on magnetic MOFs, and in particular on combining physical property characterization (e.g., magnetic susceptibility, heat capacity) with X-ray charge-density methods to obtain a microscopic understanding of the macroscopic material properties [10,11]. In studies of magnetic MOFs, it is of interest to construct non-magnetic reference systems that are isostructural to the magnetic systems [12,13], and it was during such efforts

*Corresponding author. Fax: +45 8619 6199.
E-mail addresses: hfanoe@chem.au.dk (H.F. Clausen), rdp@chem.au.dk (R.D. Poulsen), adb@chem.sdu.dk (A.D. Bond), marie@chem.au.dk (M.-A.S. Chevallier), bo@chem.au.dk (B.B. Iversen).

0022-4596/$ - see front matter © 2005 Elsevier Inc. All rights reserved.
doi:10.1016/j.jssc.2005.08.013

that we obtained the present Zn-based MOFs. Zn-based MOFs have indeed been the focus of many recent studies [14–18]. We report here two new crystal structures derived from the Zn–terephthalic acid (benzene-1,4-dicarboxylic acid, H_2BDC)–dimethyl formamide (DMF) system. Previously, Yaghi and co-workers have obtained the so-called MOF-2, $Zn(BDC)(DMF)(H_2O)$ [19], and MOF-5, $Zn_4O(BDC)_3(DMF)_8(C_6H_5Cl)$ [20], from the comparable system by room-temperature crystallization. The MOF-5 structure has been characterized both with solvent molecules in the voids (DMF, C_6H_5Cl) and fully desolvated, i.e., $Zn_4O(BDC)_3$ [20]. In a particularly thorough study, Wright and co-workers [21] have shown that different structures can be obtained from these basic reactants, and that some of the structures can be reversibly interconverted. New crystalline structures were also obtained when the basic amorphous "ZnBDC" structure was treated with different hydrogen-bonding solvents, demonstrating that the solvent molecules must be considered in "framework formation rather than inclusion into pre-existing frameworks" [21]. The Yaghi and Wright studies have also shown that identical crystal structures (MOF-2) obtained in different laboratories can exhibit different gas sorption properties.

In contrast to the previous studies, we have used solvothermal synthesis. It has often been observed that variation of the solvothermal process conditions (pressure, temperature, time, concentration) can produce different materials from the same reactants. The two new structures described here reiterate that the synthetic control and stereochemical understanding of MOF systems is challenging, and the metastable nature of one of the products demonstrates that kinetic factors can play an important role in the self-assembly of MOFs.

2. Experimental

2.1. Synthesis

A solution of benzene-1,4-dicarboxylic acid (2 mmol, 0.324 g) in DMF (8 mL) was added to a solution of $Zn(NO_3)_2 \cdot 6H_2O$ (2 mmol, 0.582 g) in DMF (2 mL). The mixture was heated in an autoclave for 4 days at 381 K. Cooling of the vessel to room temperature resulted at first in two types of macroscopically similar colourless single crystals (**1** and **2**) suitable for X-ray analysis. The sample was kept in the solvent due to sensitivity to exposure in air. The synthesis batch was re-examined after 12 months, and a single crystal of MOF-2 was picked from the solution.

2.2. Crystallographic data collection and refinement

To examine the purity of the bulk sample, X-ray diffraction data were measured on an STOE powder diffractometer at the Department of Chemistry, University of Aarhus, using Ge(111)-monochromated Cu $K\alpha_1$ radiation. The powder X-ray diagram reveals that several crystalline phases are present immediately after the synthesis. After 12 months, a new powder X-ray diagram was recorded, which showed substantial changes. The crystal structures of **1** and **2** were solved first, whereas our analysis of MOF-2 was undertaken 1 year later. All three crystals have similar crystal habits.

Due to the air-sensitive nature of the crystals, they were mounted in protective oil and transferred rapidly to a cold N_2 gas stream. For compounds **1**, $Zn(C_8H_4O_4)(C_3H_7NO)$, and **2**, $Zn(HCO_2)_3(C_2H_8N)$, colourless crystals were analysed using a Bruker-Nonius X8 APEXII diffractometer at the Department of Chemistry, University of Southern Denmark. For MOF-2, $Zn(C_8H_4O_4)(C_3H_7NO)(H_2O)$, data were collected on a similar instrument at the Department of Chemistry, University of Aarhus. For **1** and **2**, the temperature was kept at 180(2) K, and for MOF-2 at 100(2) K. Our collection of diffraction data at 100 K allows some comments to be made regarding the thermal variation of the MOF-2 structure, see Section 3.4. In each case, the data collections used combinations of ω- and ϕ-scans with step widths of 0.3–0.5°. The data were integrated using the *SAINT* program [22], and normalizations, empirical absorption corrections and averaging of the data sets were carried out with the program *SADABS* [22]. The structures were solved using the direct methods program *SHELXS* [23], and refined against F^2 data using *SHELXL* [23]. All H atoms bound to C atoms were placed in calculated positions and allowed to ride during subsequent refinement. The H atoms of the water molecule in MOF-2 were located in difference Fourier maps and refined without restraint with isotropic displacement parameters. Experimental and refinement details are summarized in Table 1, and the atomic coordinates for the three structures are given in the Supplementary material. Crystallographic data (excluding structure factors) have been deposited with the Cambridge Crystallographic Data Centre as supplementary publications CCDC-266351 (**1**), CCDC-266350 (**2**) and CCDC-271518 (MOF-2 at 100 K). Copies of these data can be obtained free of charge on application to CCDC, 12 Union Road, Cambridge CB2 1EZ, UK (fax: +44 1223 336033; e-mail: deposit@ccdc.cam.ac.uk).

3. Results and discussion

3.1. Crystal structure of *1*

The structure of **1** contains carboxylate-bridged pairs of Zn^{2+} ions interconnected by BDC linkers, forming a continuous 2-D network parallel to the $(\bar{4}02)$ planes, Fig. 1. A DMF molecule is bonded directly to Zn^{2+} (Zn(1)–O(10)), modelled as disordered over two equally populated sites across a crystallographic mirror plane. The coordination geometry around Zn(1) is a distorted square pyramid, common for Zn^{2+} with coordination number five [24]. The angles are distorted by up to 13° from regular square-pyramidal geometry, and Zn(1) lies 0.36 Å above the basal plane, see Table 2. The Zn···Zn distance of

Table 1
Crystallographic and experimental details

	1	**2**	MOF-2
Empirical formula	$Zn(C_8H_4O_4)(C_3H_7NO)$	$Zn(HCO_2)_3(C_2H_8N)$	$Zn(C_8H_4O_4)(C_3H_7NO)(H_2O)$
Formula weight	302.58	246.52	320.59
Z	4	6	4
Temperature (K)	180(2)	180(2)	100(2)
Wavelength (Å)	0.71073	0.71073	0.71073
Crystal system	Monoclinic	Trigonal	Monoclinic
Space group	$C2/m$	$R\bar{3}c$	$P2_1/n$
a (Å)	11.1369(5)	8.1818(1)	6.6456(2)
b (Å)	14.0217(7)	8.1818(1)	15.2232(5)
c (Å)	7.9890(4)	22.1235(7)	12.6148(4)
β (deg.)	106.316(1)	90	104.110(2)
V (Å^3)	1197.3(1)	1282.57(5)	1237.70(7)
ρ_{calc} (g cm^{-3})	1.679	1.915	1.720
Crystal size (mm^3)	$0.20 \times 0.20 \times 0.10$	$0.12 \times 0.12 \times 0.05$	$0.15 \times 0.15 \times 0.10$
μ (mm^{-1})	2.063	2.872	1.933
$N_{measured}$	3148	2358	33664
N_{unique}	1372	356	5919
$(\sin\theta/\lambda)_{max}$	0.6621	0.6667	0.8003
R_{int}	0.0461	0.0219	0.0357
N_{obs} $[I>2\sigma(I)]$	1223	335	4608
N_{par}	104	26	180
R_1 $[I>2\sigma(I)]$	0.060	0.014	0.048
wR_2 (all data)	0.169	0.039	0.100
GoF	1.27	1.11	1.07

2.945(2) Å is typical of that observed in comparable carboxylate-bridged dinuclear species (average 2.94(5) Å from 12 structures in the Cambridge Structural Database [25]).

Adjacent Zn(BDC)(DMF) layers stack with an offset that allows the DMF ligands from adjacent layers to fill the voids in the primary layer. The phenyl rings of the BDC linkers are twisted ca 28(1)° with respect to the two carboxylate groups, to accommodate the DMF molecules in these voids, Fig. 2. The displacement ellipsoids of C(3) and C(4) have enlarged components perpendicular to the plane of the phenyl ring, suggesting that the magnitude of the twist is slightly variable between different BDC molecules, or that there is some dynamic motion.

3.2. Crystal structure of **2**

Structure **2** consists of Zn^{2+} interconnected by deprotonated formic acid moieties (HCO_2^-) to form a 3-D framework with stoichiometry $[Zn(HCO_2)_3]_n^{n-}$, Fig. 3. The anionic formate moiety is a decomposition product of the reactant DMF. The structure is a Zn^{2+} analogue of dimethylammonium copper(II) formate [26]. The coordination geometry of the six oxygen atoms around Zn^{2+} is approximately octahedral, with a 1.3° maximum deviation in the bond angles from a regular octahedron, see Table 3. Dimethylammonium cations, $(CH_3)_2NH_2^+$, are located in the voids of the framework, also derived from decomposition of DMF. These are modelled as disordered about a site of 32 (D_3) point symmetry. The electrostatic interactions between the anionic framework and cationic solvent molecules are augmented by hydrogen bonding: the one unique H atom of the NH_2^+ group in the dimethylammonium cation lies 2.02 Å from the nearest oxygen atom in the framework (N(1)···O(1) = 2.885(3) Å, N(1)–H(1A)···O(1) = 161°), Fig. 3c.

3.3. Crystal structure of MOF-2 at 100 K

To assist the subsequent comparison, a brief description of the MOF-2 structure (at 100 K) is given here. The structure comprises 2-D layers with connectivity identical to those in compound **1**, but with water molecules axially coordinated to Zn^{2+}, rather than DMF. The coordination geometry around each individual Zn^{2+} ion is closely comparable to that in **1**, see Table 4. The 2-D layers in MOF-2 are stacked with bifurcated hydrogen bonds formed from the water molecule to the oxygen atoms of two different carboxylate groups, Fig. 4c (O(5)···O(2) = 2.963(3) Å, O(5)···O(3) = 2.996(3) Å). The DMF molecules are located within the voids in the planes of the 2-D layers, accepting shorter (non-bifurcated) hydrogen bonds from the water molecule (O(5)···O(6) = 2.594(3) Å, O(5)–H(2)···O(6) = 176.8(2)°).

3.4. Comparison of the structures of **1** and MOF-2

Comparison of the structures of **1** and MOF-2 is facilitated most readily by transforming the coordinate systems so that the 2-D layers Zn(BDC)(X) (X = DMF in **1**

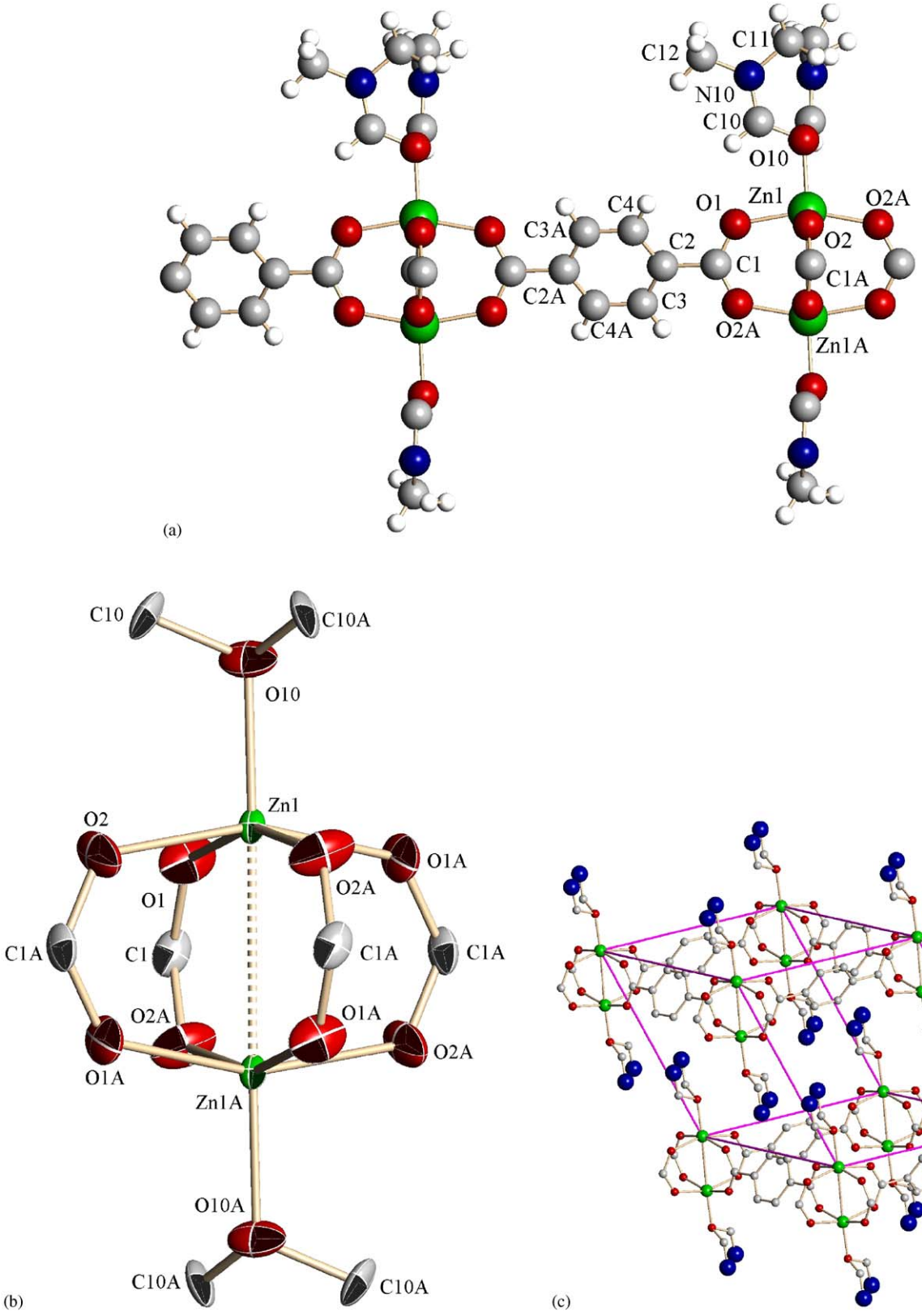

Fig. 1. (a) 2-D layer structure of compound **1** with atom numbering. (b) Central coordination sphere around the Zn atoms with ellipsoids drawn at the 50% probability level. Note the local D_{4h} point symmetry of the Zn_2O_8 unit. (c) 3-D framework with blue atoms depicting the DMF disorder. The methyl groups and one hydrogen atom have been omitted for clarity.

Table 2
Selected bond lengths (Å) and bond angles (deg.) for **1**

Zn(1)–O(1)	2.014(4)	C(1)–O(1)	1.256(8)
Zn(1)–O(2)	2.042(5)	C(1)^{iii}–O(2)	1.248(8)
Zn(1)–O(10)	2.000(7)	C(1)–C(2)	1.507(8)
Zn(1)–O(1)^{i}	2.014(4)	C(2)–C(3)	1.378(9)
Zn(1)–O(2)^{i}	2.042(5)	C(2)–C(4)	1.367(10)
Zn(1)···Zn(1)^{ii}	2.945(2)	C(3)–C(4)^{iv}	1.368(9)
O(10)–Zn(1)–O(1)	103.1(2)	C(1)–O(1)–Zn(1)	128.6(4)
O(10)–Zn(1)–O(2)	97.3(2)	C(1)^{iii}–O(2)–Zn(1)	125.5(4)
O(10)–Zn(1)–Zn(1)^{ii}	176.8(2)	C(4)–C(2)–C(3)	118.2(6)
O(1)–Zn(1)–O(1)^{i}	85.1(3)	C(4)–C(2)–C(1)	119.9(6)
O(1)–Zn(1)–O(2)	89.8(2)	C(3)–C(2)–C(1)	121.9(6)
O(1)–Zn(1)–O(2)^{i}	159.6(2)	C(4)^{iv}–C(3)–C(2)	121.6(6)
O(1)–Zn(1)–Zn(1)^{ii}	79.1(2)	C(2)–C(4)–C(3)^{iv}	120.2(6)
O(2)–Zn(1)–O(2)^{i}	88.1(4)	O(2)^{iii}–C(1)–O(1)	125.7(6)
O(2)–Zn(1)–Zn(1)^{ii}	80.5(2)	O(2)^{iii}–C(1)–C(2)	117.7(5)
		O(1)–C(1)–C(2)	116.6(6)

Symmetry transformations: (i) x, $-y$, z; (ii) $1-x$, $-y$, $1-z$; (iii) $1-x$, y, $1-z$; (iv) $\frac{1}{2}-x$, $\frac{1}{2}-y$, $-z$.

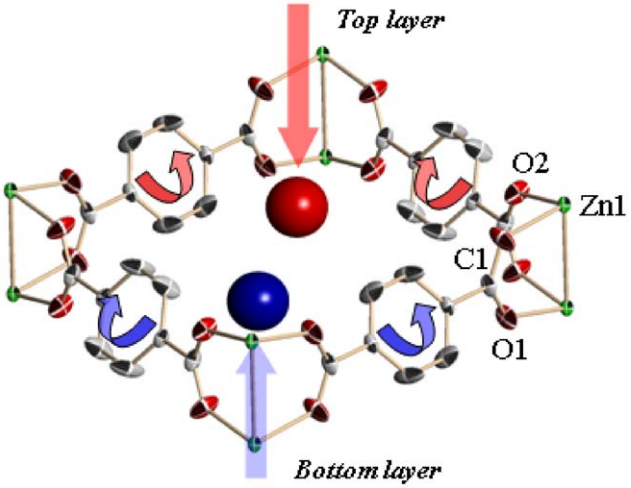

Fig. 2. Twists of the benzene rings in **1** due to the DMF molecules approaching from the adjacent layers. The displacement ellipsoids are at a 50% probability level.

and H_2O in MOF-2) lie parallel to the *ab*-plane of the unit cell. The transformed unit-cell parameters and space groups for **1**, MOF-2 at 100 K and the MOF-2 structures of Yaghi and co-workers [19] and Wright and co-workers [21] are given in Table 5. Of the two room-temperature MOF-2 structures, that of Wright is of higher precision and is used to provide the values in the following discussion.

Although the layers have comparable connectivity in **1** and MOF-2, their geometrical differences are highlighted clearly by the *a* and *b* parameters of the transformed unit cells. In **1**, the layers are rectangular and centred (the *C*-centring), while in MOF-2, they are much closer to square (but are not centred on account of a different alignment for the central Zn_2O_8 moiety, Fig. 5). The areas of the *ab*-planes in each case are closely comparable (234.4–239.5 Å^2), indicating that the difference reflects simply the

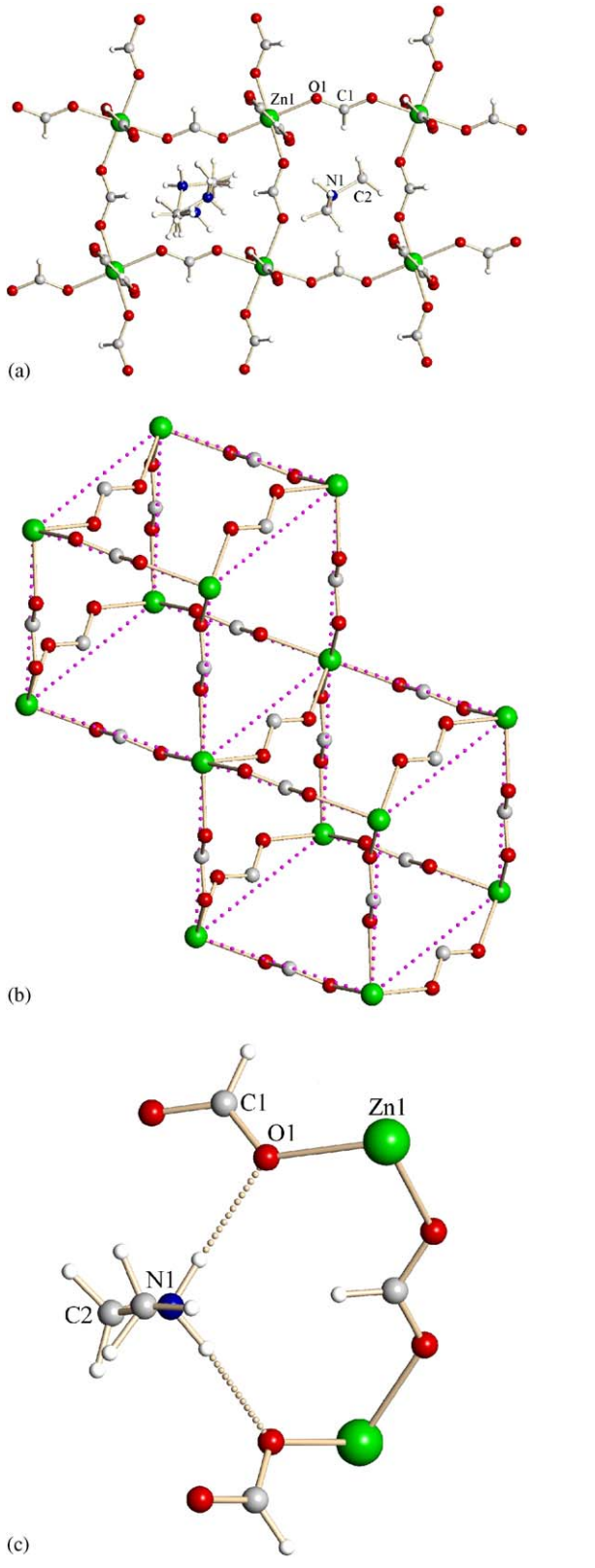

Fig. 3. (a) Layer of the framework structure of **2** showing the solvent molecules located in the voids. In the left void, the solvent disorder is shown, and in the right void one out of three solvent positions is shown. (b) 3-D framework structure. (c) Hydrogen bonds between the solvent and the framework.

Table 3
Selected bond lengths (Å) and bond angles (deg.) for **2**

Zn(1)–O(1)	2.1072(7)
C(1)–O(1)	1.2493(10)
$O(1)^{i}$–Zn(1)–O(1)	91.30(3)
$O(1)^{i}$–Zn(1)–$O(1)^{ii}$	88.70(3)
O(1)–Zn(1)–$O(1)^{ii}$	180.0
$O(1)^{i}$–Zn(1)–$O(1)^{iii}$	180.0
C(1)–O(1)–Zn(1)	126.15(9)
$O(1)^{vi}$–C(1)–O(1)	125.1(2)

Symmetry transformations: (i) $-y, x-y, z$; (ii) $-x, -y, -z$; (iii) $y, y-x, -z$; (iv) $\frac{1}{3}+x-y, \frac{2}{3}-y, \frac{1}{6}-z$.

Table 4
Selected bond lengths (Å) and bond angles (deg.) for MOF-2 at 100(2) K

Zn(1)–$Zn(1)^{ii}$	2.9389(5)	O(1)–C(7)	1.235(3)
Zn(1)–O(1)	2.010(2)	O(2)–C(7)	1.242(3)
Zn(1)–$O(2)^{ii}$	2.049(2)	C(1)–C(7)	1.502(3)
Zn(1)–$O(3)^{iii}$	2.055(2)	C(6)–C(1)	1.398(3)
Zn(1)–$O(4)^{i}$	2.017(2)	C(1)–C(2)	1.396(3)
Zn(1)–O(5)	1.960(2)	C(2)–C(3)	1.390(3)
		C(5)–C(6)	1.389(3)
O(5)–Zn(1)–O(1)	102.46(8)	C(4)–C(3)	1.399(3)
O(5)–Zn(1)–$O(2)^{ii}$	98.39(7)	C(5)–C(4)	1.398(3)
O(5)–Zn(1)–$O(3)^{iii}$	97.68(7)	C(8)–C(4)	1.501(3)
O(5)–Zn(1)–$O(4)^{i}$	103.59(7)	O(3)–C(8)	1.234(3)
O(5)–Zn(1)–$Zn(1)^{ii}$	169.97(5)	O(4)–C(8)	1.238(3)
O(1)–Zn(1)–$O(2)^{ii}$	158.61(8)		
O(1)–Zn(1)–$O(3)^{iii}$	87.6(1)	C(7)–O(1)–Zn(1)	126.8(2)
O(1)–Zn(1)–$O(4)^{i}$	91.3(1)	C(7)–O(2)–$Zn(1)^{ii}$	130.4(2)
O(1)–Zn(1)–$Zn(1)^{ii}$	81.44(6)	O(1)–C(7)–O(2)	124.0(2)
$O(4)^{i}$–Zn(1)–$O(2)^{ii}$	88.4(1)	O(1)–C(7)–C(1)	118.2(2)
$O(4)^{i}$–Zn(1)–$O(3)^{iii}$	158.43(8)	O(2)–C(7)–C(1)	117.8(2)
$O(4)^{i}$–Zn(1)–$Zn(1)^{ii}$	85.42(6)	C(2)–C(1)–C(6)	119.7(2)
$O(2)^{ii}$–Zn(1)–$O(3)^{iii}$	85.0(1)	C(2)–C(1)–C(7)	119.2(2)
$O(2)^{ii}$–Zn(1)–$Zn(1)^{ii}$	77.21(6)	C(6)–C(1)–C(7)	121.1(2)
$O(3)^{iii}$–Zn(1)–$Zn(1)^{ii}$	73.10(6)	C(3)–C(2)–C(1)	120.6(2)
		C(2)–C(3)–C(4)	119.8(2)
		C(5)–C(4)–C(3)	119.6(2)
		C(5)–C(4)–C(8)	120.7(2)
		C(3)–C(4)–C(8)	119.8(2)
		C(6)–C(5)–C(4)	120.6(2)
		C(5)–C(6)–C(1)	119.7(2)
		C(8)–O(3)–$Zn(1)^{iv}$	136.1(2)
		C(8)–O(4)–$Zn(1)^{v}$	121.3(2)
		O(3)–C(8)–O(4)	123.9(2)
		O(3)–C(8)–C(4)	117.2(2)
		O(4)–C(8)–C(4)	118.9(2)

Symmetry transformations: (i) $\frac{1}{2}-x, \frac{1}{2}-y, \frac{1}{2}-z$; (ii) $-x, 1-y, 1-z$; (iii) $x-\frac{1}{2}, \frac{1}{2}-y, \frac{1}{2}+z$; (iv) $\frac{1}{2}+x, \frac{1}{2}-y, z-\frac{1}{2}$; (v) $\frac{1}{2}-x, y-\frac{1}{2}, \frac{1}{2}-z$.

degree of rectangular distortion of the layers. The geometrical variation is accommodated by the framework in two ways. First, the geometry of the Zn_2O_8 unit differs between **1** and MOF-2. In **1**, the Zn_2O_8 unit has essentially regular D_{4h} point symmetry,[1] see Fig. 1, with both Zn^{2+} ions lying on the local four-fold rotation axis. In MOF-2, there is a lateral distortion that is accompanied by tilting of the BDC linkers with respect to the basal planes of the ZnO_5 square pyramids, see Fig. 4a. The direction of this lateral distortion is perpendicular in adjacent Zn_2O_8 units within each layer (i.e., there is not a concerted lateral distortion of each layer). Secondly, the BDC linkers themselves undergo some distortion from planarity: O(1), O(2), O(3) and O(4) lie 0.01, 0.10, 0.07 and 0.19 Å, respectively, from the least-squares plane defined by the phenyl ring C(1)–C(6).

The Zn(BDC)(*X*) layers in both **1** and MOF-2 stack along the *c*-axis of the transformed unit cells, with a perpendicular separation between layers (defined as $c\sin(180–\beta)$) that is similar in the two cases: 5.11 Å for **1** and 5.20 Å for MOF-2 at 100 K. However, the magnitude of the layer offset is significantly different in the two structures. The offset can be defined to lie parallel to the *a*-axis of the transformed unit cells, and is given by $c\cos(180–\beta)$. In MOF-2, the offset is relatively small, ca 4.13 Å. This accommodates the bifurcated hydrogen bonds between the water molecule bonded to Zn^{2+} in one layer, and the O atoms of the carboxylate groups in the adjacent layer. The lateral distortion of the Zn_2O_8 units in MOF-2 serves to reduce the O···O distances between layers, so that formation of the hydrogen bond appears to provide some driving force for the distortion. In **1**, the offset of adjacent layers is much greater, ca 6.14 Å. This accommodates the DMF molecules bonded to Zn^{2+} in one layer, i.e., the larger offset allows these molecules to project into the voids within the adjacent Zn(BDC)(DMF) layers. In MOF-2, where these coordinated DMF moieties are not present, the voids within each layer are occupied by non-coordinated DMF solvent molecules.

The unit-cell volume of MOF-2 contracts by ca 30 $Å^3$ between room temperature and 100 K. The perpendicular separation between layers (5.33 Å at room temperature) decreases by ca 0.1 Å at 100 K, while the lateral offset between adjacent layers (4.18 Å at room temperature) remains largely unaffected by the temperature change. The most significant variation with temperature lies in the bifurcated interlayer O–H···O hydrogen bond formed from the water molecule to the O atoms of the carboxylate groups: at room temperature, the bifurcated interaction is essentially symmetrical (the O(5)···O(2) and O(5)···O(3) distances of 3.00 Å do not differ significantly), while at 100 K the interaction becomes moderately, but significantly, asymmetrical. The shortened hydrogen bonds lie parallel to the BDC linkers lying along one direction of the square 2-D layers, so that the offset of adjacent layers is ca 0.3 Å greater parallel to this direction compared to the perpendicular direction. This change in the offset of the layers is accompanied by a small distortion of the layers themselves towards rectangular, suggesting that the layer geometry is correlated—at least to some degree—with formation of this interlayer hydrogen bond.

[1]The actual crystallographic $2/m$ (C_{2h}) point symmetry is a consequence of the twists of the phenyl rings of the BDC units away from co-planarity with the carboxylate groups.

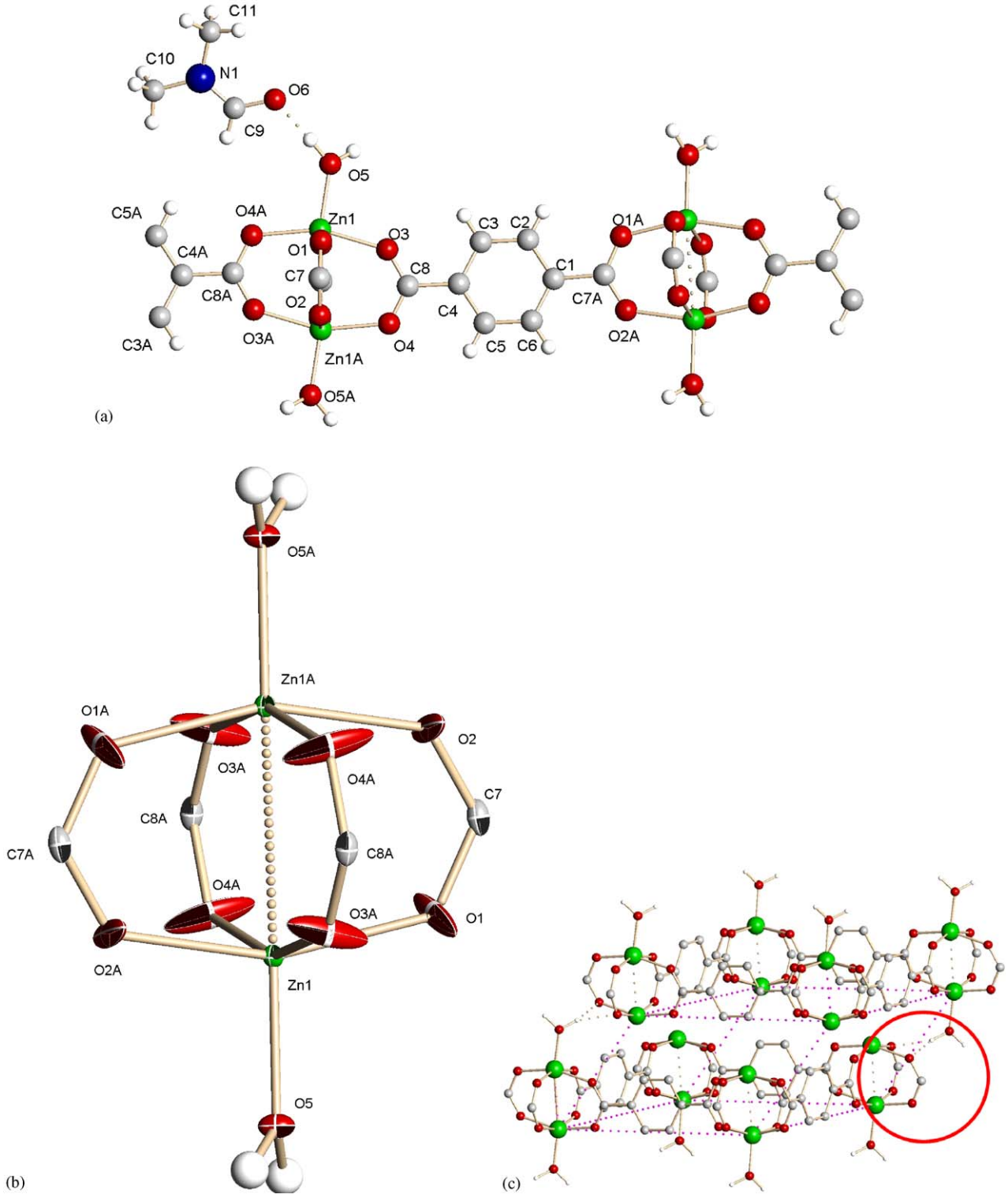

Fig. 4. (a) 2-D layer structure of MOF-2 with atom numbering. Note the distortion of the Zn_2O_8 units from local D_{4h} point symmetry. (b) Central coordination sphere around the Zn atoms is shown with ellipsoids drawn at the 50% probability level. (c) Layer structure of MOF-2. All Zn atoms have axial water ligands, but some have been omitted for clarity. Solvent DMF molecules are also omitted. The circle highlights the bifurcated hydrogen bond formed between the water molecule and carboxylate groups in adjacent layers.

3.5. Conversion of *1* to MOF-2

It is interesting that the crystal habits of **1**, **2** and MOF-2 are very similar and that the three crystal specimens were obtained ultimately from the same synthesis batch. The powder X-ray diffraction (PXRD) pattern measured immediately after the synthesis reveals that the bulk sample comprises almost exclusively **1**, Fig. 6. The phase **2** is not

Table 5
Details of the structure transformations for **1** and MOF-2

	1	MOF-2 (100 K)	MOF-2 (Yaghi) [19]	MOF-2 (Wright) [21]
Space group	$C2/m$	$P2_1/n$	$P2_1/n$	$P2_1/n$
a (Å)	11.1369(5)	6.6456(2)	6.718(3)	6.7334(3)
b (Å)	14.0217(7)	15.2232(5)	15.488(7)	15.5158(7)
c (Å)	7.9890(4)	12.6148(4)	12.430(8)	12.4532(6)
β (deg.)	106.316(1)	104.110(2)	102.83(4)	102.795(1)
V (Å^3)	1197.3(1)	1237.70(7)	1261(1)	1268.7(2)
Transformation matrix	$\begin{pmatrix} 1 & 0 & 2 \\ 0 & -1 & 0 \\ 0 & 0 & -1 \end{pmatrix}$	$\begin{pmatrix} -1 & 0 & 1 \\ 0 & -1 & 0 \\ 1 & 0 & 0 \end{pmatrix}$	$\begin{pmatrix} -1 & 0 & 1 \\ 0 & -1 & 0 \\ 1 & 0 & 0 \end{pmatrix}$	$\begin{pmatrix} -1 & 0 & 1 \\ 0 & -1 & 0 \\ 1 & 0 & 0 \end{pmatrix}$
Transformed structure				
Space group	$C2/m$	$P2_1/a$	$P2_1/a$	$P2_1/a$
a (Å)	16.714	15.626	15.386	15.438
b (Å)	14.022	15.223	15.488	15.516
c (Å)	7.989	6.646	6.718	6.773
β (deg.)	140.25	128.47	128.03	128.13

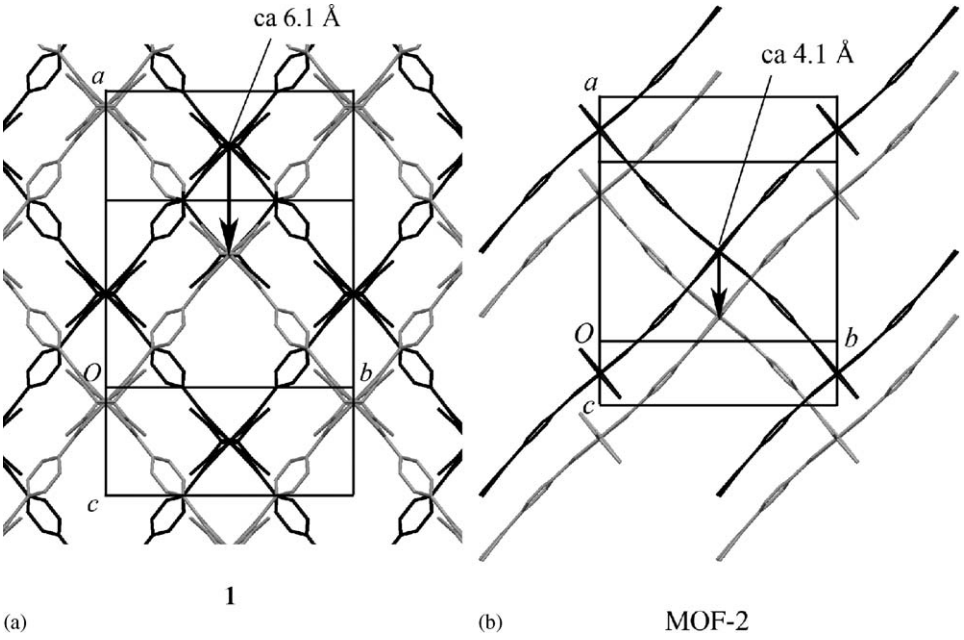

Fig. 5. Projection onto the plane of the layers in the transformed structures, illustrating the different layer offsets in 1 and MOF-2. The lower layer is shaded black and the upper layer is shaded grey.

visible, demonstrating that the single crystal picked from solution is far from representative of the bulk. Two broad peaks at ca 14° and 21° remain unaccounted for, suggesting the presence of an additional unknown phase with low crystallinity. There is no evidence of MOF-2 at this stage. After 12 months, the PXRD pattern shows that MOF-2 is the dominant phase, and there is no evidence of **1**, Fig. 6. In addition, peaks corresponding to **2** are now visible. This is likely to reflect the apparent loss of crystallinity of the MOF-2 phase compared to **1**—the absolute intensity of the diffraction pattern from MOF-2 is considerably less than that from **1** so that diffraction from phase **2** becomes apparent (e.g., the peak at $2\theta = 20°$). Since phase **2** relies on decomposition of DMF to produce formic acid moieties, it is unlikely to increase after the initial synthesis. The PXRD patterns demonstrate that the principal product of the solvothermal synthesis is the kinetic (metastable) product **1**, which converts completely to the thermodynamic product MOF-2 over a period of 12 months. The phase **2**, derived from decomposition of the DMF moieties, is a minor phase that remains stable over 12 months.

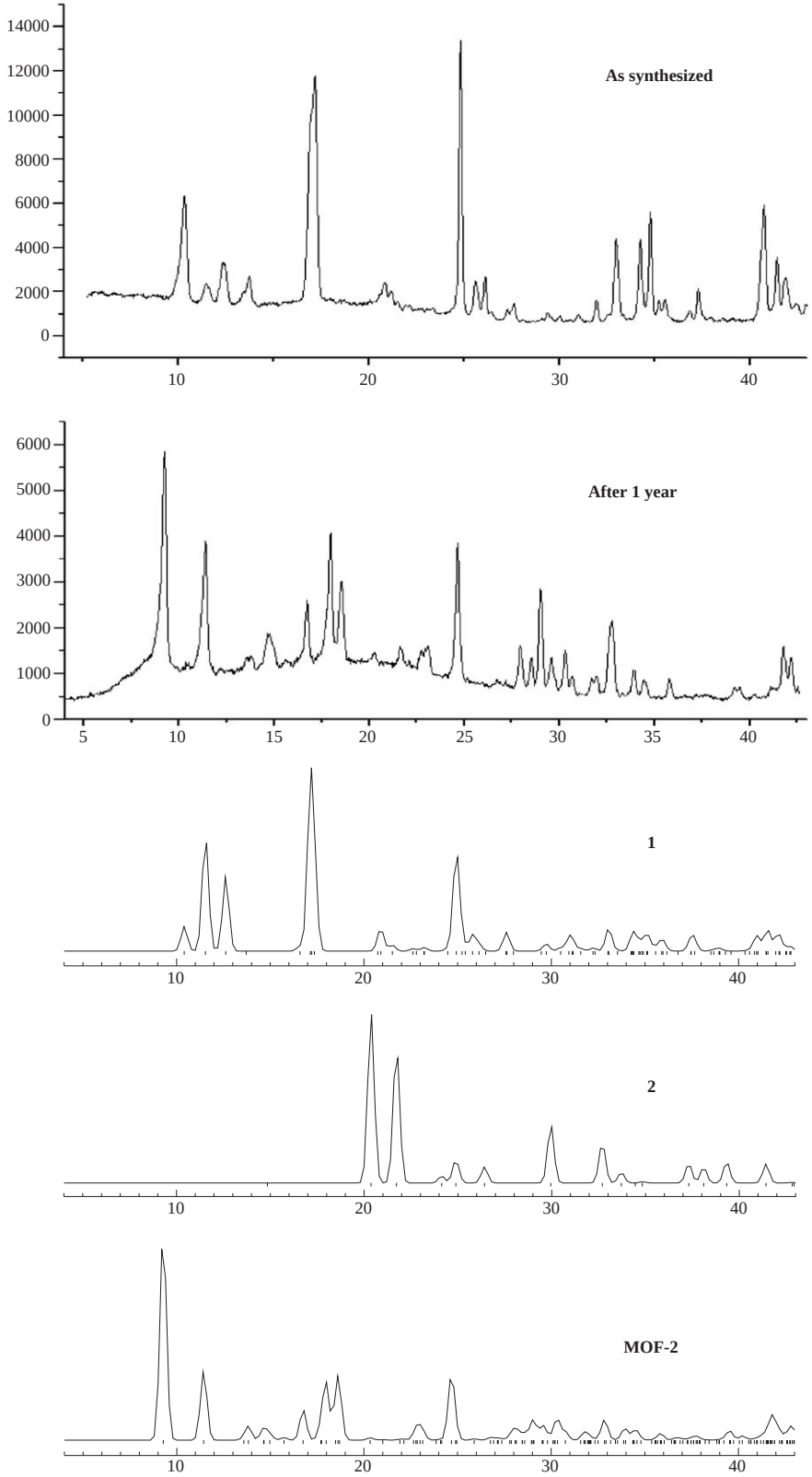

Fig. 6. X-ray powder diffraction diagrams of the initial synthesis product and after 12 months. The theoretical patterns refer to compound **1**, **2** and MOF-2. Note that the unit cells used for indexing are measured at 180, 180 and 293 K for **1**, **2** and MOF-2, respectively, whereas the powder data are recorded at room temperature.

4. Conclusion

Solvothermal synthesis has produced two new crystal structures derived from the Zn–terephthalic acid–DMF system. The major synthesis product is the metastable $Zn(C_8H_4O_4)(C_3H_7NO)$, **1**, which converts completely over a period of 12 months to the known crystalline phase MOF-2, the phase obtained by crystallization at ambient conditions [19,21]. Thus, solvothermal synthesis in this MOF system produces metastable products under kinetic control. An additional phase, $Zn(HCO_2)_3(C_2H_8N)$, **2**, is also produced, derived from decomposition of the DMF moieties, demonstrating clearly the risks for undesired reactant decomposition under these solvothermal conditions. The phase **2** is stable over the 12-month period. The study demonstrates that MOF syntheses can produce not only multiple crystal structures under different conditions, but also numerous different structures, including some that are metastable, under identical conditions.

Appendix A. Supplementary materials

Supplementary data associated with this article can be found in the online version at doi:10.1016/j.jssc.2005.08.013

References

[1] S. Kitagawa, R. Kitaura, S. Noro, Angew. Chem. Int. Ed. 43 (2004) 2334–2375.
[2] J.Y. Lu, Coord. Chem. Rev. 246 (2003) 327–347.
[3] M. O'Keeffe, M. Eddaoudi, H. Li, T. Reineke, O.M. Yaghi, J. Solid State Chem. 152 (2000) 3–20.
[4] O.M. Yaghi, M. O'Keeffe, N. Ockwig, H.K. Chae, M. Eddaoudi, J. Kim, Nature 423 (2003) 705–714.
[5] O.M. Yaghi, H. Li, C. Davis, D. Richardson, T.L. Groy, Acc. Chem. Res. 31 (1998) 474–484.
[6] M. Eddaoudi, D. Moler, H. Li, T.M. Reineke, M. O'Keeffe, O.M. Yaghi, Acc. Chem. Res. 34 (2001) 319–330.
[7] M. Eddaoudi, J. Kim, N. Rosi, D. Vodak, J. Wachter, M. O'Keeffe, O.M. Yaghi, Science 295 (2002) 469–472.
[8] H.K. Chae, D.Y. Siberio-Pérez, J. Kim, Y. Go, M. Eddaoudi, A.J. Matzger, M. O'Keeffe, O.M. Yaghi, Nature 427 (2004) 523–527.
[9] N. Rosi, M. Eddaoudi, D. Vodak, J. Eckert, M. O'Keeffe, O.M. Yaghi, Science 300 (2003) 1127–1129.
[10] R.D. Poulsen, A. Bentien, T. Graber, B.B. Iversen, Acta Crystallogr. A 60 (2004) 382–389.
[11] R.D. Poulsen, A. Bentien, M. Chevalier, B.B. Iversen, J. Am. Chem. Soc. 127 (2005) 9156–9166.
[12] E. Tynan, P. Jensen, N.R. Kelly, P.E. Kruger, A.C. Lees, B. Moubaraki, K.S. Murray, J. Chem. Soc. Dalton Trans. (2004) 3440–3447.
[13] R.D. Poulsen, A. Bentien, M. Christesen, B.B. Iversen, Acta Crystallogr. B, submitted.
[14] H. Li, C.E. Davis, T.L. Groy, D.G. Kelley, O.M. Yaghi, J. Am. Chem. Soc. 120 (1998) 2186–2187.
[15] S.-Y. Yang, Z.-G. Sun, L.-S. Long, R.-B. Huang, L.-S. Zheng, Main Group Met. Chem. 25 (2002) 579–580.
[16] L.-N. Zhu, L.Z. Zhang, W.-Z. Wang, D.-Z. Liao, P. Cheng, Z.-H. Jiang, S.-P. Yan, Inorg. Chem. Commun. 5 (2002) 1017–1021.
[17] N.L. Rosi, J. Kim, M. Eddaoudi, B. Chen, M. O'Keeffe, O.M. Yaghi, J. Am. Chem. Soc. 127 (2005) 1504–1518.
[18] T. Loiseau, H. Muguerra, G. Férey, M. Haouas, F. Taulelle, J. Solid State Chem. 178 (2005) 621–628.
[19] H. Li, M. Eddaoudi, T.L. Groy, O.M. Yaghi, J. Am. Chem. Soc. 120 (1998) 8571–8572.
[20] H. Li, M. Eddaoudi, M. O'Keeffe, O.M. Yaghi, Nature 402 (1999) 276–279.
[21] M. Edgar, R. Mitchell, A.M.Z. Slawin, P. Lightfoot, P.A. Wright, Chem. Eur. J. 7 (2001) 5168–5175.
[22] G. M. Sheldrick, SAINT, Version 7.06a and SADABS, Version 2.10 within APEX2, Version 1.0-22, Bruker-Nonius B.V., Delft, The Netherlands, 2004.
[23] G.M. Sheldrick, SHELXTL, Version 6.10, Bruker AXS Inc., Madison, WI, USA, 2000.
[24] F.A. Cotton, G. Wilkinson, C.A. Murillo, M. Bochmann, Advanced Inorganic Chemistry, Wiley, New York, 1999.
[25] F.H. Allen, Acta Crystallogr. B 58 (2002) 380–388 (CSD November 2004 release plus February 2005 and May 2005 updates (347763 entries in total)).
[26] E. Sletten, L.H. Jensen, Acta Crystallogr. B 29 (1973) 1752–1756.